

## Shape Transformation of Gold Nanoparticles from Octahedron to Cube Depending on *in situ* Seed-Growth Time

Mijin Kim, Hyung Ju Park,<sup>†</sup> Sang Woo Han,<sup>‡</sup> Jimin Park,<sup>§</sup> and Wan Soo Yun<sup>§,\*</sup>

Korea Research Institute of Standards and Science (KRISS), Daejeon 305-600, Korea

<sup>†</sup>Electronics and Telecommunications Research Institute (ETRI), Daejeon 305-700, Korea

<sup>‡</sup>Department of Chemistry, KAIST, Daejeon 305-701, Korea

<sup>§</sup>Department of Chemistry, Sungkyunkwan University (SKKU), Suwon 440-746, Korea. \*E-mail: wsyun87@skku.edu

Received April 5, 2013, Accepted May 10, 2013

**Key Words :** Gold nanoparticles, Shape transformation, *In situ* seed-growth

Synthesis of shape-controlled metal nanoparticles has been intensively studied due to their shape-dependent material properties.<sup>1-5</sup> In particular, gold nanoparticles have received a great attention due to their usefulness in optical, chemical, and biological applications.<sup>3,6-9</sup> Various shapes of gold nanoparticles, such as cubes, octahedrons, rods, and branched multipods have been prepared in a high yield using seed-mediated method which provides better control over the shape and size distribution of the nanoparticles.<sup>10-17</sup>

In this study, we report on the observation that the particle shape was dependent upon *in situ* seed-growth time of our one pot synthesis of gold nanoparticles. It was found that the cube yield increased with the increase of the seed-growth time while a short seed-growth time (~15 min) resulted in the formation of high-yield octahedral particles. This can also be regarded as a simple and convenient method of synthesizing octahedral and cubic gold nanoparticles in aqueous solution. Although the synthetic methods using cetyltrimethylammonium bromide (CTAB) and ascorbic acid have been previously reported, the shape control of gold nanoparticles relied on the adjustment of the concentration of reducing agent, gold precursor, activators, or seed particles. In this report, shape of gold nanoparticles was controlled by tuning only one parameter, the *in situ* seed-growth time, without any variation in reactant concentrations or in the way of a separate seeding.

Typically, a 250  $\mu\text{L}$  of 10 mM  $\text{HAuCl}_4 \cdot 3\text{H}_2\text{O}$  solution was added to a 20 mL of 10 mM CTAB aqueous solution. After the solution was gently mixed, 100  $\mu\text{L}$  of 100 mM L-ascorbic acid was added to this solution and mixed thoroughly. The color of the resulting solution changed from yellow to colorless and the mixture was left to stand for 30 min to reduce  $\text{Au}^{3+}$  to  $\text{Au}^+$  sufficiently and then 30  $\mu\text{L}$  of 100 mM NaOH was carefully injected to the bottom of the reaction vessel. The mixtures were left undisturbed for seed particles to form and grow for different periods of time (*in situ* seed-growth time). The solutions were then mixed thoroughly after the period of time.

As shown in Figure 1, the seed-growth time influenced the shape of gold nanoparticles. It is well-known that the interaction between the faceting tendency of the stabilizing agent

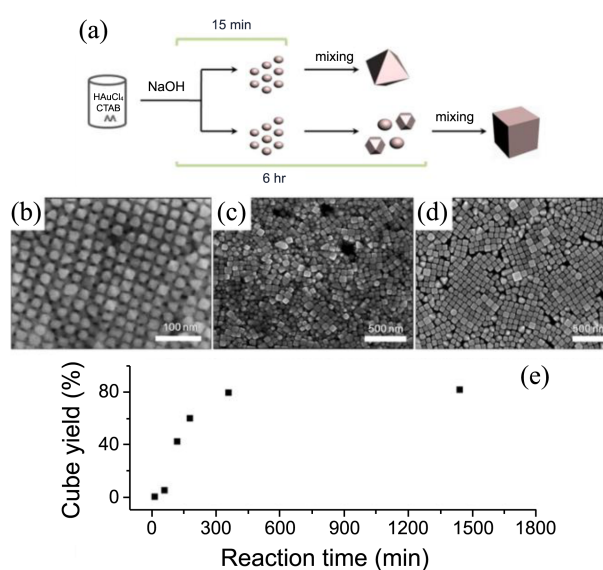


**Figure 1.** Schematic illustration of the growth process that we propose to account for the formation of octahedral and cubic gold nanoparticles and FESEM images of Au nanoparticles synthesized under different seed-growth time conditions: ((b): 15 min, (c): 2 h, and (d): 6 h). The yield of cubic gold nanoparticles at different seed-growth time (e).

and the rate of  $\text{Au}^0$  supply to the crystallographic planes is important for the formation of various shapes.<sup>14</sup> Generally, the shape control of nanoparticles of an fcc crystal is related to their surface energies associated with different facets which increase in the order of  $\gamma_{\{111\}} < \gamma_{\{100\}} < \gamma_{\{110\}}$ .<sup>2</sup> However, stabilizing agent can interact selectively with different metal crystal facets and alter their surface energies. In case of CTAB, it prefers the  $\{100\}$  facets to the  $\{111\}$  facets.

As described before, gold nanoparticles were synthesized by mixing an aqueous solution of  $\text{HAuCl}_4$ , CTAB, and ascorbic acid, followed by the addition of NaOH into the reaction mixture. NaOH was added into the reaction mixture as an activator producing the  $\text{Au}^0$  atoms through the reduction of  $\text{Au}^+$  ions,<sup>11</sup> since the ascorbic acid only converts  $\text{Au}^{3+}$  ions into  $\text{Au}^+$  ions.<sup>18</sup> Careful addition of NaOH to the bottom part is a crucial step in obtaining the monodispersed

gold nanoparticles. After adding the NaOH, small seed particles were gradually formed at the bottom of the reaction vessel, which was noticeable from the advent of a reddish color at the bottom layer (Figure S1). This step with the retarded mixing can be regarded as a control of the local concentration of NaOH by manipulating its flux. For the synthesis of octahedral nanoparticles, the solution was mixed well for dispersing the small seed particles generated after 15 min from the NaOH injection. This mixing step can exert very similar effect on the reaction as the addition of seed particles prepared separately. The dispersed small seed particles will provide the active sites for metal ion reduction, which leads to the faster formation of Au<sup>0</sup> atoms. At this condition, octahedrons wrapped by thermodynamically more stable {111} facets were obtained. On the other hand, when the reaction mixture was left to stand for a long time without mixing, cubic gold nanoparticles were obtained. In this condition, the preferred binding of CTAB on {100} facets may induce a directed addition of gold atoms onto the {111} facets, which increases the yield of the cubic nanoparticles surrounded by CTAB-stabilized {100} facets.

Figure 1(b), 1(c), and 1(d) are the representative field emission scanning electron microscopy (FESEM) images of gold nanoparticles. The morphology and cube yield depend on the *in situ* seed-growth time. When the seed-growth time was given for 15 min, monodispersed octahedral gold nanoparticles were obtained (Figure 1(b)). As shown in Figure 1(b), the orderly assembled gold nanoparticles obtained after solvent evaporation, reflecting the uniformity of the particles. With the increase of the seed-growth time, the yield of cubic nanoparticles, the cube yield, increased and upon an extended seed-growth ( $\geq 6$  h) the major product was the cubic nanoparticles. Figure 3 shows the dependence of the cube yield upon the seed-growth time. The cube yield increased with the increase of the seed-growth time until 6 h starting from almost zero at  $\sim 15$  min. Further increase of the seed-growth did not improve the cube yield whose maximum was about 80% (Figure 1(e)).

One can find that the cubic nanoparticles are less homogeneous in size compared with the octahedral nanoparticles (Figure 1(d)). This can be attributed to the inhomogeneous environment of the bottom layer due to the interface between the bottom (seed-growing) and the upper (remaining) layer. Close to the interface, the seed-growth in the bottom layer may be affected by the upper layer whose chemical composition is different from the bottom layer. Actually, the two layers are almost fully mixed after 6 h of the seed-growth time (Figure S1). Therefore, it can be inferred that the crystal growth has taken place along with a retarded mixing of the solution by diffusion of the reactants, to which the size distribution of the cubic gold nanoparticles can be attributed.

Morphology of the seed particles formed right after the seed-growth period was also inspected by TEM taking an aliquot before the additional mixing. The shape of particles taken after 15 min was nearly spherical having an average diameter of 10 nm. However, in the case of the sample taken

after 6 h, several shapes were mixed (Figure S2). Although the cubic nanoparticles were not monodispersed, they were yet quite homogeneous in size and were obtained in a quite high yield. It was also found that the sizes of cubic nanoparticles were relatively larger than those of octahedral ones, which could be attributed to the Ostwald ripening which might also affect the size distribution.

In conclusion, we have found a strong dependence of particle shape upon *in situ* seed-growth time which basically is the interval for the delayed mixing of the whole reagents. The yield of cubic gold nanoparticles increased with increase of the *in situ* seed-growth time, while octahedral nanoparticles were the major product when the time was relatively short. This observation, therefore, can also be considered as a simple method to selectively synthesize octahedral and cubic gold nanoparticles in high yields without the separate steps for seed preparation.

**Acknowledgments.** This work is supported by the National Research Foundation funded by the MEST, Korea (2012-0009565 and NRF-2012-M3C1A1-048860).

**Supporting Information.** Optical images, TEM images, UV/vis spectra and HRTEM images with an electron diffraction pattern are available at the journal webpage.

## References

1. Tao, A. R.; Habas, S.; Yang, P. *Small* **2008**, *4*, 310.
2. Sun, Y.; Xia, Y. *Science* **2002**, *298*, 2176.
3. Tran, T.; Nguyen, T. *Colloids Surf. B* **2011**, *88*, 1.
4. Xia, Y.; Xiong, Y.; Lim, B.; Skrabalak, S. E. *Angew. Chem. Int. Ed.* **2009**, *48*, 60.
5. Lim, J.; Lee, S.; Yoon, S. *Bull. Korean Chem. Soc.* **2011**, *32*, 4113.
6. Sanchez-Iglesias, A.; Pastoriza-Santos, I.; Perez-Juste, J.; Rodriguez-Gonzalez, B.; Liz-Marzan, L. M. *Adv. Mater.* **2006**, *18*, 2529.
7. Maiorano, G.; Rizzello, L.; Malvindi, M. A.; Shankar, S. S.; Martiradonna, L. M.; Falqui, A.; Cingolani, R.; Pompa, P. P. *Nanoscale* **2011**, *3*, 2227.
8. Kim, W. J.; Choi, S. H.; Rho, Y. S.; Yoo, D. J. *Bull. Korean Chem. Soc.* **2011**, *32*, 4171.
9. Kim, H.; Chandra, S. L.; Jang, J. *Bull. Korean Chem. Soc.* **2007**, *51*, 407.
10. Grzelczak, M.; Perez-Juste, J.; Mulvaney, P.; Liz-Marzan, L. M. *Chem. Soc. Rev.* **2008**, *37*, 1783.
11. Seo, D.; Yoo, C. I.; Park, J. C.; Park, S. M.; Ryu, S.; Song, H. *Angew. Chem., Int. Ed.* **2008**, *47*, 763.
12. Ma, Y.; Kuang, Q.; Jiang, Z.; Xie, Z.; Huang, R.; Zheng, L. *Angew. Chem. Int. Ed.* **2008**, *47*, 8901.
13. Millstone, J. E.; Wei, W.; Jones, M. R.; Yoo, H.; Mirkin, C. A. *Nano Letters* **2008**, *8*, 2526.
14. Chen, L.; Leong, G. J.; Schulze, M.; Dinh, H. N.; Pivovar, B.; Hu, J.; Qi, Z.; Fang, Y.; Prikhodko, S.; Pozuelo, M.; Kodambaka, S.; Richards, R. M. *ChemCatChem* **2012**, *4*, 1662.
15. Xiao, J.; Qi, L. *Nanoscale* **2011**, *3*, 1383.
16. Zhang, J.; Langille, M. R.; Personick, M. L.; Zhang, K.; Li, S.; Mirkin, C. A. *J. Am. Chem. Soc.* **2010**, *132*, 14012.
17. Niu, W.; Zheng, S.; Wang, D.; Liu, X.; Li, H.; Han, S.; Chen, J.; Tang, Z.; Xu, G. *J. Am. Chem. Soc.* **2009**, *131*, 697.
18. Murphy, C. J.; Sau, T. K.; Gole, A. M.; Orendorff, C. J.; Gao, J.; Gou, L.; Hunyadi, S. E.; Li, T. *J. Phys. Chem. B* **2005**, *109*, 13857.